UGP2, a novel target gene of TP53, inhibits endothelial cells apoptosis and atherosclerosis

Xin He
Zhujiang Hospital
Juan-Jiang Chen
Zhujiang Hospital
Xiu-Mei Hu
Nanfang Hospital
Chang-Meng Wu
Nanfang Hospital
Ru-Yi Zhang
Nanfang Hospital
Biao Yang
Zhujiang Hospital
Lei Zheng
Nanfang Hospital
Qian Wang (wangqian@smu.edu.cn)
Zhujiang Hospital

Research Article

Keywords: UGP2, TP53, ROS, apoptosis, atherosclerosis.

Posted Date: June 3rd, 2022

DOI: https://doi.org/10.21203/rs.3.rs-1658149/v2

Abstract

Dysfunction of the endothelial lining of lesion-prone areas of the arterial vasculature is an important contributor to the pathobiology of atherosclerotic cardiovascular disease. Recent studies have indicated that UDP-glucose pyrophosphorylase 2(UGP2) is implicated in cell proliferation and survival. Here we investigated the anti-apoptosis and anti-atherogenic effect of UGP2 in vitro and in vivo.Here, we explored the effects and mechanisms of UGP2 on apoptosis in endothelial cells by flow cytometer and Western blot analyses. And we engineered $ldlr^{-/-}ugp2^{+/-}$ double-deficient mice to evaluated the apoptosis levels in atherosclerotic lesion. A microarray analysis showed that the expression of UGP2 was reduced in human atherosclerotic plaques. In vitro experiments revealed that TP53 interacted with the promotor region of the UGP2 gene, which upregulated UGP2 expression. Augmentation of UGP2 expression downregulated ROS levels, the expressions of Cleaved caspase-3 and apoptosis levels in endothelial cells, and this inhibitory effects of UGP2 on cell apoptosis could be significantly abolished by H_2O_2. In vivo experiments using $ldlr^{-/-}ugp2^{+/-}$ mice fed a Western high-fat diet demonstrated that UGP2 deficiency promoted atherosclerosis, and increased the levels of ROS, expressions of Cleaved caspase-3 and apoptosis cells in atherosclerotic lesions. Thus, our results provide evidence for UGP2 as a novel target gene of TP53 contributes to anti-apoptosis effect linking to ROS homeostasis differ from canonical pathway, and we suggested that UGP2 could act as potential therapeutic targets to ameliorate atherosclerosis-related diseases.

1. Introduction

Atherosclerosis (AS) is the main pathogeny of coronary heart disease, cerebral infarction and peripheral vascular disease, and that endothelial dysfunction (ED) is suggested as one of the early events in the pathogenesis of atherosclerotic progression[1]. Endothelial cells have important roles in normal physiological processes including the secretion of chemokines and cell adhesion factors, regulating vascular relaxation and contraction, and promoting angiogenesis[2–5]. However, when pathological conditions arise causing apoptosis, the important biological functions maintained by the endothelium become compromised. Due to impaired barrier function of the endothelium, infiltration of the vascular wall by circulating leukocytes in combination with increased low-density lipoprotein (LDL) storage initiates the development of atherosclerosis[6, 7].

UGP2 also known as UDP–glucose pyrophosphorylase is an enzyme involved in carbohydrate metabolism. Its significance is derived from the many uses of UDP-glucose including galactose metabolism, glycogen synthesis, glycoprotein synthesis, and glycolipid synthesis[8, 9]. A deficiency in this enzyme during the glycogen synthesis and decomposition processes leads to the clinical manifestations of glycogen storage disease[10]. UGP2 has been identified with tumor-specific alternative transcription start sites (TSSs) in both adenoma and cancer samples relative to normal mucosa[11]. High transcript levels of UGP2 were identified in acute myeloid leukemia (AML) and were associated with significantly poor overall survival in AML[12]. UGP2 was enriched in the biological progresses of cell proliferation, migration, and invasion and positively correlated with pathologic grade, both in hepatocellular

carcinoma[13, 14] and glioma[15]. These studies showed that the UGP2 expression level was significantly higher in cancer cells than in the corresponding normal cells or tissue. It has also been shown that hypoxia induces UGP2 expression[16]. The expression of UGP2 and its association with the clinicopathological characteristics of atherosclerosis have not been reported.

TP53 is a transcription factor activated upon DNA damage and inhibits cell proliferation by inducing cell cycle arrest, senescence or apoptosis[17, 18]. TP53 exerts these actions principally via binding to the consensus binding motifs in the genome, thereby activating the transcription of its target genes. It has been known that, among the target genes, p21 mediates cell cycle arrest[19] while apoptosis is mediated by Bax, NOXA, Pidd or PUMA[20–23]. However, recent studies challenge these long-held views of TP53 function. Recent evidences suggest that TP53 influences a range of cellular metabolic processes, including glycolysis, glutaminolysis and anti-oxidant response. In contrast to its role in promoting apoptosis during DNA damaging stress, TP53 can promote cell survival during metabolic stress. In these conditions, TP53 protects cells from oxidative stress directly by inducing anti-oxidant genes, like GPX1, ALDH4 or indirectly by regulating glucose and glutamine metabolism related protease, like TIGAR and GLS2[24–27]. these metabolizing enzymes have been identified as a family of TP53-inducible proteins that provide an antioxidant defense to protect cells from apoptosis by decrease intracellular ROS[28]. The antioxidant role of TP53 is important to reduce oxidative stress-induced DNA damage and mutations, which contributes greatly to the cell survival. Cell survival regulated by TP53 plays a central role in atherosclerosis. Some research revealed that transplant of TP53 bone marrow to $tp53^{-/-}$ mice reduced aortic plaque formation and reduced VSMCs apoptosis in brachiocephalic plaques[29, 30]. And Rajan et al [31] found that TP53 inhibits cardiomyocyte apoptosis and protects infarct myocardium under some conditions.

Here, we identify UGP2 as a TP53 target gene to mediate the role of TP53 in antioxidant defense mechanisms. TP53 increases UGP2 expression, which results in decreased ROS levels, endothelial cell survival and inhibitory effect of atherosclerosis. These results suggest that UGP2 is an important component in the cell survival and anti-atherosclerosis effects of TP53.

2. Materials And Methods

2.1 Tissues

In this study, 10 patients with atherosclerotic plaque and normal arterial tissues were all from atherosclerotic patients who underwent carotid endarterectomy at Southern Hospital of Southern Medical University. Arteries without macroscopic evidence of atherosclerosis were collected from individuals who died from a traffic accident or cerebral edema. After washing the specimens with saline, the outer fat tissues and surrounding normal tissues of the plaque were separated. The plaque tissue was separated into appropriate sizes, and immediately placed in liquid nitrogen. The collected tissue was pathologically tested and diagnosed as primary atherosclerosis. The exclusion criteria were patients with diabetes, cancer, congestive heart failure, valvular heart disease, hematological system diseases, autoimmune

disease, and/or infections. The basic information of the patients included name, age, and sex. The study was approved by the Committee for Ethical Review of Research Involving Human Subjects, Nanfang Hospital, Southern Medical University, Guangzhou, China (Ethics approval ID: NFEC-2018-142). Informed consent was obtained from the participants or relatives of deceased individuals.

2.2 Cells

Human vascular endothelial cells (HUVECs, ATCC CRL-1730) were obtained from ATCC. HUVECs were cultured in Dulbecco's modified Eagle's medium (DMEM) containing 10% fetal calf serum (FCS). The cells were incubated at 37°C in an atmosphere of 5% CO_2. Cells were seeded in 6- or 12-well plates or 60 mm dishes and grown to 60–80% confluence before use.

2.3 Animals

$ldlr^{-/-}$ mice and $ugp2^{+/-}$ mice were purchased from the Model Animal Research Center of Nanjing University (Nanjing, China). All experimental protocols in accordance with the NIH Guide for the Care and Use of Laboratory Animals were approved by the Ethic Committee of Nanfang Hospital, Southern Medical University. All mice had the C57BL/6J background. To generate ldlr and ugp2 double-deficient mice, $ugp2^{+/-}$ mice were crossbred with $ldlr^{-/-}$ mice. Due to embryonic lethality of ugp2-knockout homozygosity ($ugp2^{-/-}$), $ugp2^{+/-}$ $ldlr^{-/-}$ and $ugp2^{+/+}$ $ldlr^{-/-}$ mice were used in this study. Six-week-old mice from both groups (5 males and 5 females in each group) were fed a Western high-fat diet for 12 weeks. Thereafter, mice were fasted for 4 hours, then placed under general anesthesia, after which blood was collected from the retro-orbital venous plexus using a capillary tube. The mice were then sacrificed by cervical dislocation, and tissues were collected for analysis.

2.4 Quantitative RT-PCR analysis

Total RNA from cultured cells were extracted using TRIzol reagent (Invitrogen, Carlsbad, CA, USA) and reverse transcribed. Real-time PCR was performed on the lightCycler 480 II (Roche, Pleasanton, CA, USA) with SYBR Green Dye detection (TaKaRa Bio, Mountain View, CA, USA). All samples were assayed in triplicate. The data were analyzed using the ΔΔCt method, with GAPDH as a reference in the mRNA analysis. The primer sequences are listed in Table.1.

2.5 Immunoblot analysis

The total protein was measured by the bicinchoninic acid protein assay kit (P0010-1; Beyotime, China). The cleavage products of each sample were separated by 12% SDSPAGE. The western blots were incubated for 12h at 4℃ with antibodies against UGP2 (Abcam, catalog ab157473), TP53 (Abcam, catalog ab26), Cleaved caspase-3 (CST, catalog #9664), or β-ACTIN (Abcam, catalog ab8227), and then incubated 2h at room temperature with horseradish-peroxidase-conjugated secondary antibodies. Chemiluminescence (ECL Plus Western Blot Detection System; Amersham Biosciences, Foster City, CA, USA) was used in the visualization of proteins.

2.6 Detection of intracellular ROS

Intracellular generation of ROS was detected by fluorescence probe 2, 7-dichlorofluorescin diacetate kit (DCFH-DA, Sigma) as described by the production instruction. HUVECs were treated with 0.5mM H_2O_2(Sigma)for 24h after transfection. The treated cells were washed three times with PBS and then incubated in 10 mM DCFH-DA for 30 min at 37°C without light. After washed 3 times with PBS, the samples were assessed on a flow cytometer and analyzed using CellQuest (BD Biosciences, New Jersey, New York, USA) software.

2.7 Detection of apoptosis cells

Cells apoptosis was assessed using an apoptosis detection kit (Kaiji Biotechnology, Nanjing, China). Briefly, cells were collected after treatment, washed twice in ice-cold PBS, and resuspended in binding buffer, then added into 5μl of Annexin V-APC and 5μl of 7-AAD mixed for 15 min at room temperature in the dark. The samples were assessed on a flow cytometer and analyzed using CellQuest (BD Biosciences, New Jersey, New York, USA) software. Apoptotic cells were quantitated by Annexin V binding and 7-AAD uptake. The Annexin V-APC + 7-AAD– cell populations were considered to represent early apoptotic cells, and The Annexin V-APC + 7-AAD + cell populations were considered to represent lately apoptotic cells.

2.8 siRNA assay

Control siRNA (negative control), siRNA-UGP2, and siRNA-TP53 were purchased from Ribo Targets (Guangzhou, China). ECs were transfected with 50 nM siRNA. Control samples for all experimental procedures were processed with a non-targeting control mimic sequence of equal concentration. qRT-PCR and Western blotting analysis was performed to observe the efficiency of siRNA protein knockdown. The sequence of siRNA-UGP2, siRNA-TP53, and control siRNA are shown in Table.2.

2.9 Recombinant plasmid construction

A plasmid containing the full-length UGP2 cDNA was purchased from OriGene (Rockville, MD, USA). UGP2 cDNA was amplified by PCR and subcloned into the pcDNA3.1 (+) vector. The correct sequence of the UGP2 cDNA in the recombinant plasmid was verified by sequencing and named pcDNA-UGP2. The plasmid was used to transfect ECs using Lipofectamine 3000transfection reagent.

2.10 ChIP

Human vascular endothelial cells (HUVECs) were crosslinked by incubation in formaldehyde and then incubated with glycine to quench formaldehyde. ChIP was carried out using an anti-TP53 antibody (Abcam, catalog ab26) and the Pierce Agarose ChIP kit (Thermo Fisher Scientific) according to the manufacturer's instructions. DNA in the chromatin immunoprecipitated by the anti-TP53 antibody or an isotope IgG (Abcam, catalog ab172730) to serve as a control was subjected to quantitative PCR analysis of the UGP2 gene and the housekeeping gene β-ACTIN promotor sequence, respectively. The primer sequences are listed in Table.3.

2.11 Histological and immunohistochemical analyses

Sections (4μm thick) of formalin-fixed, paraffin-embedded human atherosclerotic plaques and normal arterial wall specimens, respectively, were subjected to immunohistochemical staining using an anti-UGP2 antibody (Abcam, catalog ab157473).

To examine the extent of aortic atherosclerotic lesions in the studied mice, the aorta was opened longitudinally along the ventral midline from the iliac arteries to the aortic root, pinned out flat on a blue surface, and stained en face with oil red O (Sigma-Aldrich). Images of stained aortas were captured using a Leica DMI6000 microscope. The oil red O–stained areas were quantified using Image-Pro Plus 6.0 (Media Cybernetics).

Formalin-fixed, paraffin-embedded sections (3μm thick) of mouse hearts with aortic root were stained with H&E, Masson for collagen, von Kossa for calcification, Tunel for apoptosis, and immunohistochemically stained using antibodies for Cleaved caspase-3 (CST, catalog #9664). Frozen sections (3μm thick) of mouse hearts with aortic root were stained with oil red O, and DHE for ROS. Images were acquired using an Olympus BX50 microscope with a digital color camera and analyzed using Optimus software (version 6.2).

2.12 Statistical analysis

Data were analyzed using SPSS version 13.0 (SPSS, Chicago, IL, USA) software. Data are presented as the mean ± SD or median (interquartile range) unless otherwise indicated. The results were analyzed by one-way analysis of variance or unpaired Student's t-tests when continuous variables were normally distributed. A two-tailed p value < 0.05 was considered statistically significant.

3. Results

3.1 UGP2 was decreased in atherosclerosis and inhibits cell apoptosis.

To identify differentially expressed genes in human atherosclerotic plaques, we performed microarray analysis on aortic atherosclerotic plaque tissues (from 3 patients) and healthy aortic tissues (from 3 individuals) [32], the analysis showed that the expression of UGP2 transcript was decreased. To verify that finding in microarray analysis, the immunohistochemistry analysis of samples from additional subjects confirmed that the protein levels of UGP2 were 24.2 ± 11.6% lower in atherosclerotic plaques (the carotid artery aorta from 5 patients) than in healthy arterial intima tissues (from 5 individuals) (Fig. 1a).

In order to investigate the effect of UGP2 in HUVECs, firstly we treated HUVECs with siRNA-UGP2 to downregulated the expression of UGP2, the UGP2 expression was confirmed at the mRNA level by real-time PCR (Fig. 1b) and at the protein level by western-blot assays (Fig. 1c), respectively. Then HUVECs were transfected with pcDNA-UGP2, the UGP2 mRNA levels (Fig. 1d) and protein levels (Fig. 1e) were significantly upregulated. To analyze the effect of UGP2 on the apoptosis of HUVECs, the cell apoptotic rates was detected by FACS analysis with AnnexinV-APC and 7-AAD double labeling. As shown in Fig. 1f,

the apoptotic rates of control cells were 4.2 ± 0.7%, while the apoptotic rates of UGP2 knockdown cells were 13.3 ± 2.0%. These data suggest that the deletion of UGP2 induces cell apoptosis.

3.2 UGP2 inhibits cell apoptosis by reducing ROS levels.

To explore the possible mechanism of UGP2 meditating cell apoptosis, the levels of ROS were assessed in HUVECs transfected with siRNA-UGP2 or pcDNA-UGP2. As expected, the ROS levels of UGP2 knockdown cells increased to 144 ± 12.4% compared with the control cells (Fig. 2a). In cells with upregulation of UGP2, ROS levels decreased to 66 ± 7.1% of the control cells (Fig. 2b). These results suggest that the apoptosis effect of UGP2 knockdown in HUVECs may be associated with oxidative stress.

To further analyze the cause of UGP2 downregulation-induced apoptosis, the effect of UGP2 on the apoptosis signaling pathway was determined using western blot analysis. The protein expression level of Cleaved caspase-3 was detected. The expression level of Cleaved caspase-3 in UGP2 knockdown cells was significantly higher compared with that in the control cells (Fig. 2c). Furthermore, upregulated UGP2 expression significantly reduced H_2O_2-induced Cleaved caspase-3 protein levels (Fig. 2d), whereas the UGP2 knockdown by siRNA oligo significantly increased the protein levels of Cleaved caspase-3 induced by H_2O_2 (Fig. 2c).

HUVECs with upregulated UGP2 expression or UGP2 knockdown were treated with H_2O_2 and apoptotic rates were measured. Compared with H_2O_2 induced cell apoptosis alone, the apoptotic rates of UGP2 deficient cells treated with H_2O_2 was significantly increased to 20.4 ± 0.9% (Fig. 2e). In the treatment of UGP2 upregulation, the inhibitory effect of increased UGP2 expression on apoptotic rates was abolished by H_2O_2 (Fig. 2f).

3.3 UGP2 is directly activated by TP53 in ROS reduction and apoptosis inhibition.

Given the role of TP53 in glucose metabolism, we hypothesized that TP53 regulates UGP2 transcription by direct association with chromatin. Therefore, we carried out native chromatin immunoprecipitation (ChIP) experiments, isolated DNA from immunoprecipitated complexes and followed by quantitative polymerase chain reaction (qPCR) in HUVECs. The qPCR using primers designed to the UGP2 promoter showed significant enrichment of TP53 ChIP fragments at this site compared with a Control ChIP experiment using a non-specific antibody in the place of the anti-TP53 antibody (Fig. 3a).

To test the specific relationship between TP53 and UGP2, siRNA specifically targeting TP53 was transfected into HUVECs, revealing the trend of syntropy. Transfection with TP53 siRNA resulted in reduction of UGP2 transcript and protein as measured by qPCR or western blot, respectively (Fig. 3b, c).

The levels of ROS, protein expression levels of Cleaved caspase-3 and apoptotic rates were detected in TP53 knockdown HUVECs transfected with siRNA-UGP2 or pcDNA-UGP2. Our experiment results showed that the downregulation of UGP2 increased the ROS levels (109 ± 7.0%) (Fig. 3d), Cleaved caspase-3

levels (Fig. 3f) and apoptotic rates (11.9 ± 4.1%) (Fig. 3h) which TP53 siRNA reduced in HUVECs. Conversely, the ROS levels (52 ± 3.2%) (Fig. 3e), Cleaved caspase-3 levels (Fig. 3g) and apoptotic rates (6.4 ± 0.7%) were reduced in the cells with UGP2 upregulation compared with cells treated with TP53 siRNA (Fig. 3i), suggesting that UGP2 is directly activated by TP53 in ROS reduction and apoptosis inhibition in HUVECs.

3.4 Knockdown UGP2 promotes atherosclerosis and increases cell apoptosis in vivo.

To investigate whether UGP2 plays a role in the pathogenesis of atherosclerosis, we crossbred $ugp2^{+/-}$ mice with $ldlr^{-/-}$ mice to generate $ugp2^{+/-}$ $ldlr^{-/-}$ mice ($ugp2^{-/-}$ $ldlr^{-/-}$ mice could not be generated, likely due to being embryonic lethal). Both $ugp2^{+/-}$ $ldlr^{-/-}$ mice and $ugp2^{+/+}ldlr^{-/-}$ littermates (controls) were fed a Western high-fat diet for 12 weeks. En face analysis of the aorta showed that $ugp2^{+/-}$ $ldlr^{-/-}$ mice had substantially more atherosclerosis (155.8% increase) than controls (Fig. 4a), indicating that UGP2 plays a protective role against atherogenesis.

Furthermore, histological and immunohistochemical analyses of aortic root cross sections showed that, compared with the atherosclerotic lesions in $ugp2^{+/+}ldlr^{-/-}$ mice, those in $ugp2^{+/-}$ $ldlr^{-/-}$ mice had higher lipid content (144.8% higher), reduced cap thickness (52.6% lower), lower collagen content (46.2% lower) and less calcification (66.4% lower) (Fig. 4a), suggesting a protective role of UGP2 against the development of vulnerable atherosclerotic plaques.

Further analyses showed that atherosclerotic lesions in $ugp2^{+/-}$ $ldlr^{-/-}$ mice had higher levels of Cleaved caspase-3 (89.4% higher), more apoptotic cells (120.4% higher) (Fig. 4b) and increased fluorescence of ROS (75.2% higher) (Fig. 4c) than those in $ugp2^{+/+}ldlr^{-/-}$ mice, which may contribute to the protective role of UGP2 against atherogenesis and plaque vulnerability and is in line with the aforecited results of assays of cultured human cells.

4. Discussion

Atherosclerosis is a complex arterial disease characterized by vascular wall inflammation and atherosclerotic plaque accumulation. Endothelial cells play a critical role in the development of atherosclerosis, so damage to the vascular endothelium might increase the risk of triggering the pathogenesis of atherosclerosis[1]. Our study demonstrated that reduced UGP2 expression is involved in the progression of atherosclerosis via stimulation of endothelial apoptosis in vivo and in vitro. Downregulation of UGP2 was associated with increased endothelial cells apoptosis and severe atherosclerotic plaque. With these in mind, UGP2 might be a novel molecular target for cell apoptosis and atherosclerosis.

UGP2 is an enzyme involved in the biosynthesis of glycogen by catalyzing the reaction of uridine triphosphate (UTP) and glucose-1-P to generate UDP-glucose, UDP-glucose is the activated glucose required for glycogen synthesis[33]. UGP2 has previously been identified as a marker protein in various

types of malignancies where its upregulation is correlated with a poor disease outcome[11–15]. A recent cohort study on Developmental and/or epileptic encephalopathies (DEEs) revealed that the reduction of UGP2 expression in brain cells leads to global transcriptome changes, a reduced ability to produce glycogen, alterations in glycosylation and increased sensitivity to ER stress[34]. Changes in glycosylation can modulate inflammatory responses, promote cell metastasis or regulate apoptosis[35]. ER stress can react in various ways, including the induction of the unfolded protein response (UPR) and apoptosis[36]. The endothelial cells as an effective mediator to regulate the vascular system, with roles in processes such as vascular homeostasis, cell cholesterol, and signal transduction[37]. Convincing evidence indicates that dysfunction of the endothelial cells is associated with various vascular diseases, including diabetes mellitus, arterial thrombosis and hypercholesterolemia[38]. Endothelial cells apoptosis can destroy the vascular structure, results in macrophages infiltration and lipids deposition, and finally contributes to atherogenesis[39, 40]. Our study is the first to show a role of UGP2 in the development of atherosclerosis, and confirmed that the deletion of UGP2 promotes atherosclerosis by increasing Cleaved caspase-3 expressions and apoptosis levels in HUVECs.

As an important biological modulator, ROS not only play a role in maintaining normal physiological functions but also participate in cell damage and cell death because of their highly intensive activities[41]. As one of the adverse stimuli, ROS mediates activation of Cleaved caspase-3 and cell apoptosis via multiple mechanisms such as impairing membrane integrity and causing mitochondrial damage[42, 43]. During atherogenesis, the primary process of endothelial cell dysfunction and apoptosis is accompanied by a secondary event of oxidative stress, high levels of ROS can induce oxidative stress that is closely associated with the pathogenesis of atherosclerosis[44]. Low density lipoprotein (LDL) oxidation by ROS is an early event in the development of atherosclerotic lesions[45]. In addition, ROS can lead to NF-κB activation, protein modification, and oxidative damages to other biomolecules[46]. ROS also disrupt redox-dependent signaling in the vessel wall to promote progress of atherosclerosis[47]. In the present study, the HUVECs were pre-treated by UGP2 siRNA before incubation with H_2O_2, elevation of apoptosis was found, accompanied by augmentation of ROS generation and upregulation of Cleaved caspase-3 expressions. This result indicated that ROS are indispensable for UGP2 knockdown induced apoptosis in HUVECs.

It is well-known that TP53 is a tumor-suppressor gene, playing key roles in cell cycle control and induction of apoptosis through the regulation of a battery of target genes. In response to death signals, activated TP53 regulates various genes of pro-apoptotic proteins, which are transcription-dependent or independent, leading to final cell death[20–23]. Otherwise, it has recently been shown that activated TP53 promotes cell survival and capable of anti-apoptosis ability under DNA damage by implicating in the regulation of carbohydrate metabolisms[48]. Numerous studies revealed that TP53 is also a redox-regulating transcription factor via regulation of ROS production and the expression of various metabolizing enzymes, like TIGAR and GLS2[26, 27]. TP53 also plays a central role in atherosclerosis. Convincing evidence has showed that TP53 deters the development of atherosclerosis by inhibiting DNA damage signaling in VSMCs[29]. In addition, TP53 protects the genome from oxidation by reactive

oxygen species (ROS), a major cause of DNA damage in atherosclerosis[49]. In the present study, we found that UGP2 was directly transactivated by TP53, and UGP2 knockdown increased ROS generation and Cleaved caspase-3 activation through a TP53-dependent manner in vivo. Therefore, it is highly likely that UGP2 is transactivated by TP53 in response to survival stress, contributes to ROS reduction, Cleaved caspase-3 downregulation and reduction of apoptosis in HUVECs, finally results in the inhibition of atherosclerosis.

In ldlr-knockout mice fed a Western high-fat diet, we found that targeted deletion of the UGP2 gene resulted in substantially increased atherosclerotic lesion areas, indicating a protective role of UGP2 against atherogenesis. Furthermore, we observed that the atherosclerotic lesions in ugp2-deficient mice had higher lipid content, reduced cap thickness, lower collagen contents and less calcification, all of which are hallmarks of vulnerable atherosclerotic plaques[50]. In line with the findings from HUVECs, the levels of ROS and Cleaved caspase-3 expressions was upregulated and endothelial cells apoptosis was enhanced in atherosclerotic lesions of ugp2-deficient mice. As it is well established that endothelial dysregulation and apoptosis is considered as the initiating factors in the development and pathogenesis of atherosclerosis[1]. Thus, endothelial cells apoptosis induced by UGP2 deficiency results in increased atherosclerotic lesions area and more vulnerable atherosclerotic plaques in mice.

In summary, our present study not only identified the critical glycogen metabolism enzyme UGP2 as a novel direct target of TP53, but also demonstrated a novel role of UGP2 in the regulation of apoptosis through the reduction of ROS and anti-activation of Cleaved caspase-3. Based on our current findings, further extensive studies on the function of UGP2 and glycogen metabolism might provide a clue to develop a promising strategy for atherosclerosis therapy.

Declarations

Data availability

The data that support the findings of this study are available from the corresponding author upon reasonable request.

Funding

This work was supported by the National Natural Sciences Foundation of China (Grant numbers 82072334 and 81672076)

Competing Interests

The authors have no relevant financial or non-financial interests to disclose.

Author Contributions

All authors contributed to the study conception and design. Xin He and Juan-Jiang Chen designed the study, performed most part of the experiments, analyzed and interpreted the data and wrote the manuscript. Xiu-Mei Hu, Chang-Meng Wu, Ru-Yi Zhang and Biao Yang contributed to data acquisition. Lei Zheng and Qian Wang provided financial support and guided the completion of the project. All authors read and approved the final manuscript.

Ethics approval

This study was performed in line with the principles of the Declaration of Helsinki. Approval was granted by the Committee for Ethical Review of Research Involving Human Subjects, Nanfang Hospital, Southern Medical University, Guangzhou, China.

Consent to participate

Informed consent was obtained from all individual participants included in the study.

Consent to publish

The authors affirm that human research participants provided informed consent for publication of the images in Fig. 1a.

References

1. Gimbrone MJ, Garcia-Cardena G (2016) Endothelial Cell Dysfunction and the Pathobiology of Atherosclerosis. Circ Res 118(4):620–636
2. Hartmann P, Schober A, Weber C (2015) Chemokines and microRNAs in atherosclerosis. Cell Mol Life Sci 72(17):3253–3266
3. Hartmann P et al (2016) Endothelial Dicer promotes atherosclerosis and vascular inflammation by miRNA-103-mediated suppression of KLF4. Nat Commun 7:10521
4. Doring Y et al (2017) Vascular CXCR4 Limits Atherosclerosis by Maintaining Arterial Integrity: Evidence From Mouse and Human Studies. Circulation 136(4):388–403
5. Wong BW et al (2017) Endothelial cell metabolism in health and disease: impact of hypoxia. EMBO J 36(15):2187–2203
6. Asano S et al (2017) Circulating leucocytes perpetuate stroke-induced aortic dysfunction. Exp Physiol 102(10):1321–1331
7. Gradinaru D et al (2015) Oxidized LDL and NO synthesis–Biomarkers of endothelial dysfunction and ageing. Mech Ageing Dev 151:101–113
8. Scheffler TL et al (2016) Gain of function AMP-activated protein kinase gamma3 mutation (AMPKgamma3R200Q) in pig muscle increases glycogen storage regardless of AMPK activation.Physiol Rep, 4(11)

9. Poleti MD et al (2018) Label-free quantitative proteomic analysis reveals muscle contraction and metabolism proteins linked to ultimate pH in bovine skeletal muscle. Meat Sci 145:209–219
10. Janzen NR, Whitfield J, Hoffman NJ (2018) Interactive Roles for AMPK and Glycogen from Cellular Energy Sensing to Exercise Metabolism.Int J Mol Sci, 19(11)
11. Thorsen K et al (2011) Tumor-specific usage of alternative transcription start sites in colorectal cancer identified by genome-wide exon array analysis. BMC Genomics 12:505
12. de Jonge HJ et al (2011) Gene expression profiling in the leukemic stem cell-enriched CD34 + fraction identifies target genes that predict prognosis in normal karyotype AML. Leukemia 25(12):1825–1833
13. Li Y et al (2018) Multiomics Integration Reveals the Landscape of Prometastasis Metabolism in Hepatocellular Carcinoma. Mol Cell Proteomics 17(4):607–618
14. Li S et al (2019) Transcriptome-Wide Analysis Reveals the Landscape of Aberrant Alternative Splicing Events in Liver Cancer. Hepatology 69(1):359–375
15. Zeng C, Xing W, Liu Y (2019) Identification of UGP2 as a progression marker that promotes cell growth and motility in human glioma. J Cell Biochem 120(8):12489–12499
16. Pescador N et al (2010) Hypoxia promotes glycogen accumulation through hypoxia inducible factor (HIF)-mediated induction of glycogen synthase 1. PLoS ONE 5(3):e9644
17. Chen J (2016) The Cell-Cycle Arrest and Apoptotic Functions of p53 in Tumor Initiation and Progression. Cold Spring Harb Perspect Med 6(3):a026104
18. Jiang C et al (2017) Serpine 1 induces alveolar type II cell senescence through activating p53-p21-Rb pathway in fibrotic lung disease. Aging Cell 16(5):1114–1124
19. Yang HW et al (2017) Competing memories of mitogen and p53 signalling control cell-cycle entry. Nature 549(7672):404–408
20. Chipuk JE et al (2004) Direct activation of Bax by p53 mediates mitochondrial membrane permeabilization and apoptosis. Science 303(5660):1010–1014
21. Oda E et al (2000) Noxa, a BH3-only member of the Bcl-2 family and candidate mediator of p53-induced apoptosis. Science 288(5468):1053–1058
22. Lin Y, Ma W, Benchimol S (2000) Pidd, a new death-domain-containing protein, is induced by p53 and promotes apoptosis. Nat Genet 26(1):122–127
23. Nakano K, Vousden KH (2001) PUMA, a novel proapoptotic gene, is induced by p53. Mol Cell 7(3):683–694
24. Okubo T et al (2013) p53 mutations may be involved in malignant transformation of giant cell tumor of bone through interaction with GPX1. Virchows Arch 463(1):67–77
25. Yoon KA, Nakamura Y, Arakawa H (2004) Identification of ALDH4 as a p53-inducible gene and its protective role in cellular stresses. J Hum Genet 49(3):134–140
26. Bensaad K et al (2006) a p53-inducible regulator of glycolysis and apoptosis. Cell 126(1):107–120

27. Suzuki S et al (2010) Phosphate-activated glutaminase (GLS2), a p53-inducible regulator of glutamine metabolism and reactive oxygen species. Proc Natl Acad Sci U S A 107(16):7461–7466
28. Liang Y, Liu J, Feng Z (2013) The regulation of cellular metabolism by tumor suppressor p53. Cell Biosci 3(1):9
29. Mercer J et al (2005) Endogenous p53 protects vascular smooth muscle cells from apoptosis and reduces atherosclerosis in ApoE knockout mice. Circ Res 96(6):667–674
30. Guevara NV, Chen KH, Chan L (2001) Apoptosis in atherosclerosis: pathological and pharmacological implications. Pharmacol Res 44(2):59–71
31. Gogna R et al (2013) p53's choice of myocardial death or survival: Oxygen protects infarct myocardium by recruiting p53 on NOS3 promoter through regulation of p53-Lys(118) acetylation. EMBO Mol Med 5(11):1662–1683
32. Hu YW et al (2019) Long noncoding RNA NEXN-AS1 mitigates atherosclerosis by regulating the actin-binding protein NEXN. J Clin Invest 129(3):1115–1128
33. Cheng SD, Peng HL, Chang HY (1997) Localization of the human UGP2 gene encoding the muscle isoform of UDPglucose pyrophosphorylase to 2p13-p14 by fluorescence in situ hybridization. Genomics 39(3):414–416
34. Perenthaler E et al (2019) Loss of UGP2 in brain leads to a severe epileptic encephalopathy, emphasizing that bi-allelic isoform-specific start-loss mutations of essential genes can cause genetic diseases.Acta Neuropathol,
35. Reily C et al (2019) Glycosylation in health and disease. Nat Rev Nephrol 15(6):346–366
36. Seervi M et al (2018) ROS mediated ER stress induces Bax-Bak dependent and independent apoptosis in response to Thioridazine. Biomed Pharmacother 106:200–209
37. Setyawati MI et al (2015) Understanding and exploiting nanoparticles' intimacy with the blood vessel and blood. Chem Soc Rev 44(22):8174–8199
38. Cahill PA, Redmond EM (2016) Vascular endothelium - Gatekeeper of vessel health. Atherosclerosis 248:97–109
39. Hainsworth AH, Oommen AT, Bridges LR (2015) Endothelial cells and human cerebral small vessel disease. Brain Pathol 25(1):44–50
40. Goveia J, Stapor P, Carmeliet P (2014) Principles of targeting endothelial cell metabolism to treat angiogenesis and endothelial cell dysfunction in disease. EMBO Mol Med 6(9):1105–1120
41. Lim HY et al (2014) ROS regulate cardiac function via a distinct paracrine mechanism. Cell Rep 7(1):35–44
42. Chan CM et al (2016) Methylglyoxal induces cell death through endoplasmic reticulum stress-associated ROS production and mitochondrial dysfunction. J Cell Mol Med 20(9):1749–1760
43. Li X et al (2019) ROS Induced by KillerRed Targeting Mitochondria (mtKR) Enhances Apoptosis Caused by Radiation via Cyt c/Caspase-3 Pathway. Oxid Med Cell Longev, 2019: p. 4528616

44. Stocker R, Keaney JJ (2004) Role of oxidative modifications in atherosclerosis. Physiol Rev 84(4):1381–1478
45. Maiolino G et al (2013) The role of oxidized low-density lipoproteins in atherosclerosis: the myths and the facts. Mediators Inflamm, 2013: p. 714653
46. Grimsrud PA et al (2008) Oxidative stress and covalent modification of protein with bioactive aldehydes. J Biol Chem 283(32):21837–21841
47. Sies H, Berndt C, Jones DP (2017) Oxidative Stress. Annu Rev Biochem 86:715–748
48. Humpton TJ, Vousden KH (2016) Regulation of Cellular Metabolism and Hypoxia by p53.Cold Spring Harb Perspect Med, 6(7)
49. Mercer J, Bennett M (2006) The role of p53 in atherosclerosis. Cell Cycle 5(17):1907–1909
50. Hafiane A, Plaque V (2019) Characteristics, Detection, and Potential Therapies.J Cardiovasc Dev Dis, 6(3)

Tables

Table. 1 The primer sequences used for qRT-PCR analyses

Gene Name		Primer Sequence
UGP2	F[a]	ATGTCTCAAGATGGTGCTTCTCA
	R[a]	GGTGTGCTCAAATTCATGTGATG
TP53	F	TCAGCATCTTATCCGAGTGGAA
	R	TGTAGTGGATGGTGGTACAGTCA
GAPDH	F	GCACCGTCAAGGCTGAGAAC
	R	TGGTGAAGACGCCAGTGGA

[a]: F, forward; R, reverse.

Table. 2 The sequences used for RNA interference analyses

Gene Name	Sequence
siRNA-UGP2	CACATGTAGACGAGTTCAA
siRNA-TP53	CACCATCCACTACAACTAC
Control-siRNA	TTCTCCGAACGTGTCACG

Table. 3 The primer sequences used for CHIP analyses

Gene Name		Primer Sequence	Site	bp
UGP2	F[a]	CAGGGACATTTCCGCATTGAAG	1247	166
	R[a]	TCACACATGCACACCTTGAG		
β-ACTIN	F	TGACAAGGACAGGGTCTTCC	1009	169
	R	CACCGTCCGTTGTATGTCTG		

[a]: F, forward; R, reverse.

Figures

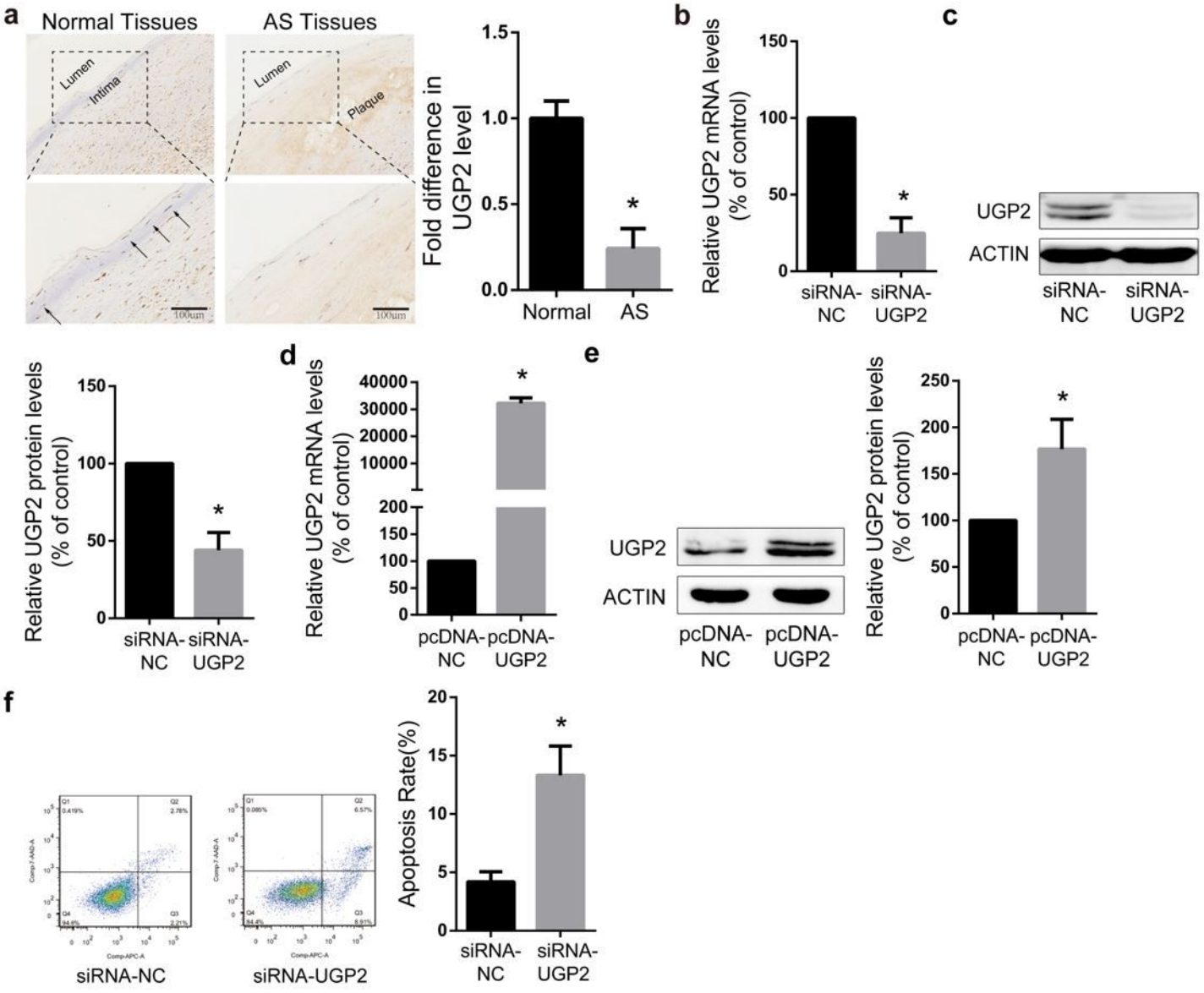

Figure 1

Reduced expression of UGP2 in human atherosclerotic plaques. (a) UGP2 protein in human normal and atherosclerotic arterial tissues, detected by immunohistochemistry. Scale bars: 100μm. AS, atherosclerotic. (b) HUVECs were transfected with the negative control or siRNA-UGP2, followed by quantitative RT-PCR analysis of UGP2 mRNA levels. (c) HUVECs were transfected with the negative control or siRNA-UGP2, followed by immunoblot analysis of the UGP2 protein levels. (d)HUVECs were transfected with the negative control or pcDNA-UGP2, followed by quantitative RT-PCR analysis of UGP2 mRNA levels. (e) HUVECs were transfected with the negative control or pcDNA-UGP2, followed by immunoblot analysis of the UGP2 protein levels. (f) HUVECs were transfected with the negative control or siRNA-UGP2, followed by FACS analysis. *$p < 0.05$. Data are represented as mean ± SD values from 3 independent experiments with each experiment done in triplicate.

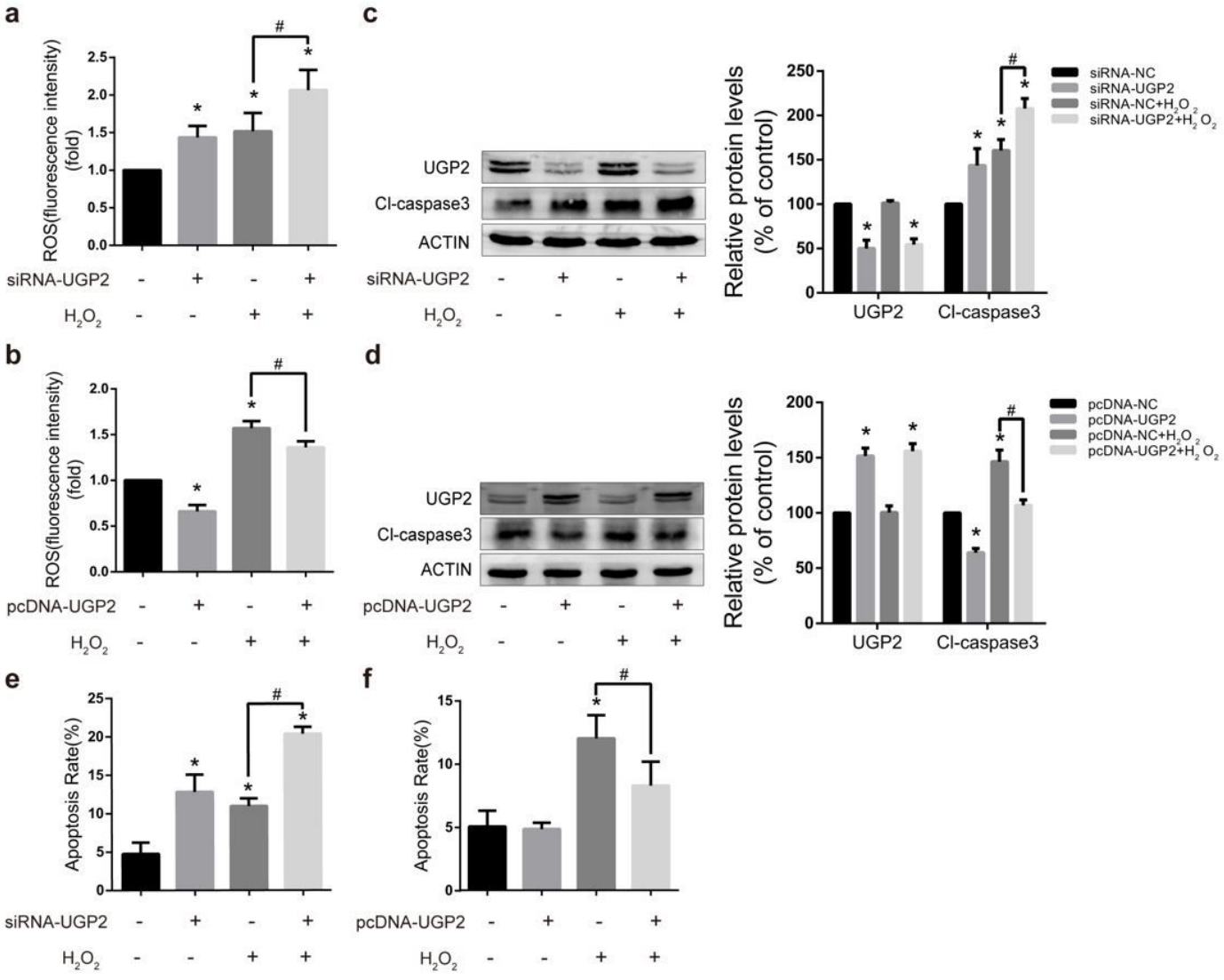

Figure 2

UGP2 suppresses cell apoptosis via ROS reduction. (a, c, e) HUVECs were transfected with the negative control or siRNA-UGP2 and then incubated with or without 0.5mM H_2O_2 for 24 h. (a) ROS levels in HUVECs were measured by FACS. (c) UGP2 and Cleaved caspase-3 protein levels in HUVECs were determined by immunoblot analysis. (e) apoptotic rates in HUVECs were measured by FACS. (b, d, f) HUVECs were transfected with the negative control or pcDNA-UGP2 and then incubated with or without 0.5mM H_2O_2 for 24 h. (b) ROS levels in HUVECs were measured by FACS. (d) UGP2 and Cleaved caspase-3 protein levels in HUVECs were determined by immunoblot analysis. (f) apoptotic rates in HUVECs were measured by FACS. *$p < 0.05$, versus control group. $^{\#}p < 0.05$, H_2O_2 group versus co-treatment group. Data are represented as mean ± SD values from 3 independent experiments with each experiment done in triplicate.

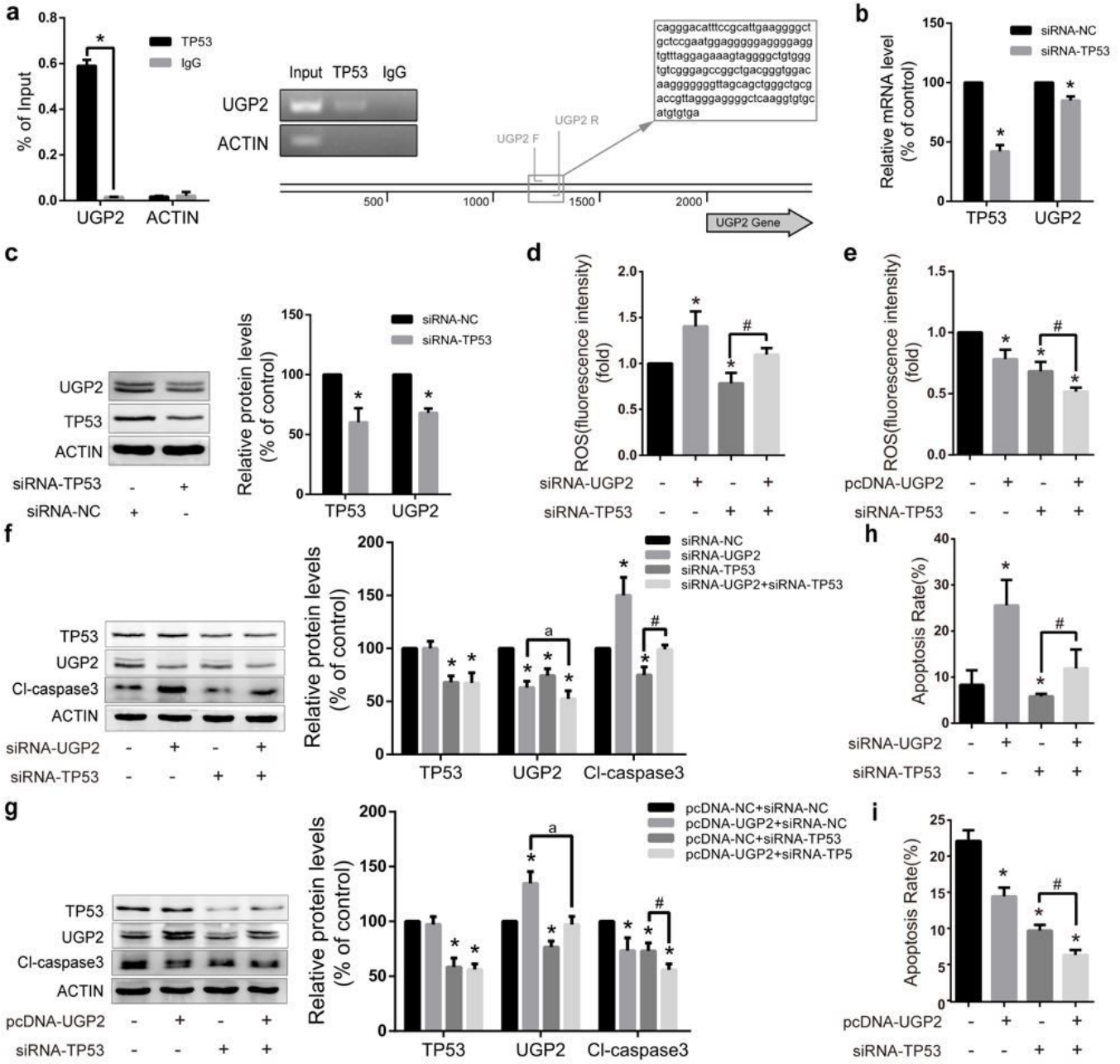

Figure 3

UGP2 is directly activated by TP53 in ROS reduction and apoptosis inhibition. (a) HUVECs were subjected to ChIP using the anti-TP53 antibody, followed by quantitative PCR analysis using primers annealing to the UGP2 promotor sequence and the housekeeping gene β-ACTIN as a reference. (b) HUVECs were transfected with the negative control or siRNA-TP53, followed by quantitative RT-PCR analysis of TP53 and UGP2 mRNA levels. (c) HUVECs were transfected with the negative control or siRNA-TP53, followed by immunoblot analysis of the TP53 and UGP2 protein levels. (d, f, h) HUVECs were co-transfected with either the negative control or siRNA-UGP2 and either TP53 siRNA or scramble (control) siRNA. (d) ROS levels in HUVECs were measured by FACS. (f) TP53, UGP2 and Cleaved caspase-3 protein levels in HUVECs were determined by immunoblot analysis. (h) apoptotic rates in HUVECs were measured by FACS. (e, g, i) HUVECs were co-transfected with the negative control or pcDNA-UGP2 and either TP53 siRNA or scramble (control) siRNA. (e) ROS levels in HUVECs were measured by FACS. (g) TP53, UGP2 and Cleaved caspase-3 protein levels in HUVECs were determined by immunoblot analysis. (i) apoptotic rates in HUVECs were measured by FACS. *$p < 0.05$, versus control group. $^{\#}p < 0.05$, siRNA-TP53 group versus co-treatment group. $^{a}p < 0.05$, pcDNA-UGP2 group versus co-treatment group. Data are represented as mean ± SD values from 3 independent experiments with each experiment done in triplicate.

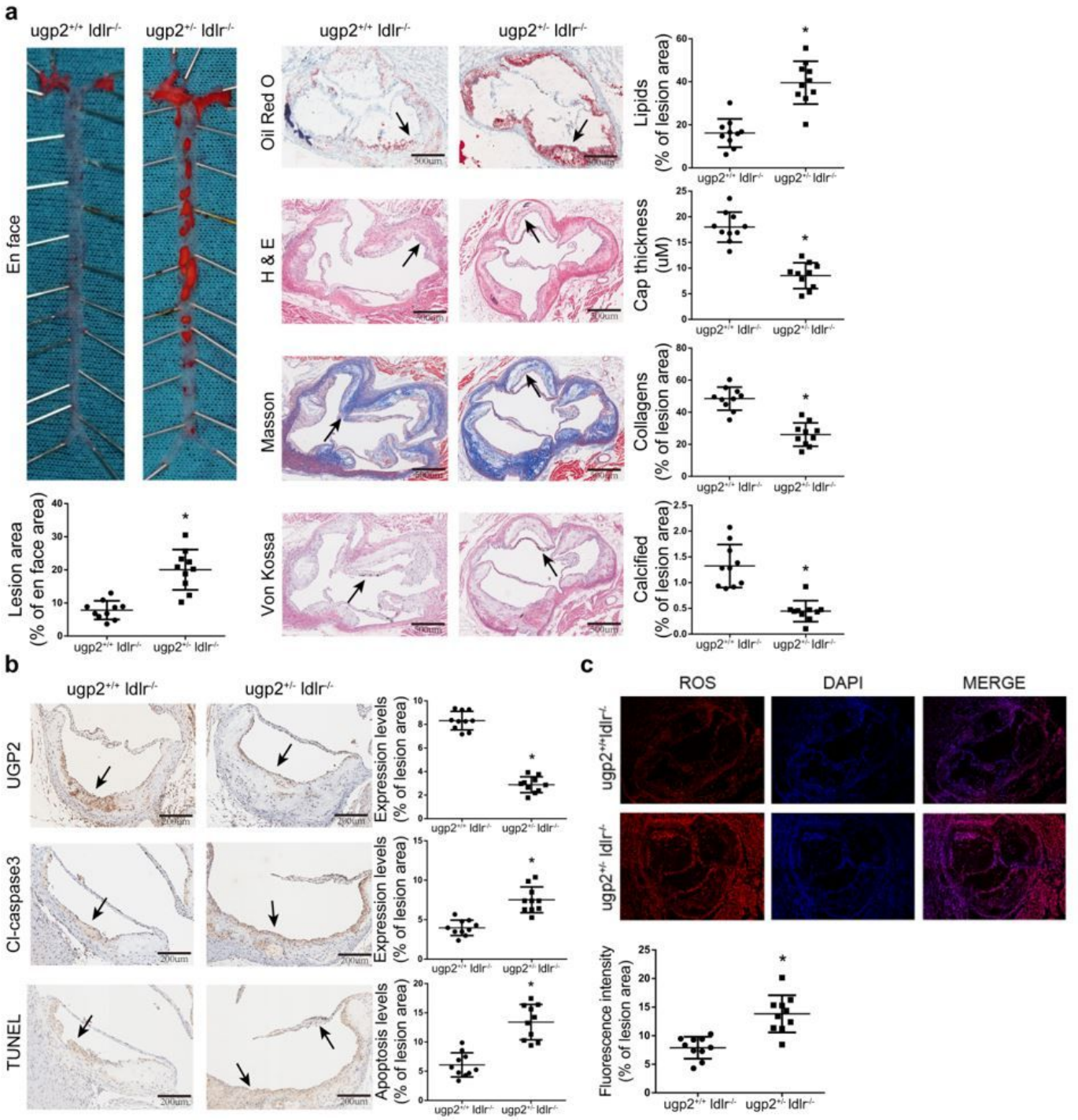

Figure 4

UGP2 deters atherosclerosis in a mouse model. ugp2$^{+/-}$ ldlr$^{-/-}$ mice and ugp2$^{+/+}$ ldlr$^{-/-}$ littermates, 6 weeks of age, were fed a Western high-fat diet for 12 weeks, followed by (a) Oil red O staining of aorta en face and H&E, Oil red O (for lipids), Masson (for collagens), Von Kossa (for calcification) staining of aortic root cross sections, respectively. Scale bars: 500μM. (b) immunohistochemical analyses of aortic root cross sections, against UGP2, and Cleaved caspase-3, respectively. TUNEL (for apoptosis) staining of aortic root cross sections. Scale bars: 200μM. (c) DHE (for ROS) staining of aortic root cross sections.

Scale bars: 500μM. *$p < 0.05$. Data are represented as mean ± SD values from 10 independent experiments.

Supplementary Files

This is a list of supplementary files associated with this preprint. Click to download.

- supplementarymaterials.rar